Semiconductor Optical Fibers for Nonlinear Applications

Anna C. Peacock[a], Li Shen[a], Fariza H. Suhailin[a,b], Natasha Vukovic[a], and Noel Healy[a]

[a]Optoelectronics Research Centre, University of Southampton, Southampton, SO17 1BJ, UK
[b]School of Fundamental Science, Universiti Malaysia Terengganu, 21300 Kuala Terengganu, Malaysia

ABSTRACT

The incorporation of semiconductor materials into the optical fiber geometry provides an important step towards enhancing the optoelectronic functionality of conventional fiber infrastructures, as well as allowing for the construction of robust devices with novel waveguiding properties. In this paper we review our progress in characterizing the nonlinear transmission properties of semiconductor optical fibers with the view to developing integrated all-optical devices. The nonlinear performance of the fibers has been benchmarked through demonstrations of high speed all-optical wavelength conversion, modulation, and continuum generation.

Keywords: Silicon Photonics, Fiber Materials, Nonlinear Optics

1. INTRODUCTION

The nascent field of semiconductor optical fibers is attracting increased interest as a means to exploit the optoelectronic functionality of the semiconductor materials directly within the fiber geometry.[1,2] Compared to their planar counterparts, this new class of waveguide retains many of the advantageous properties of the fiber platforms such as robustness, flexibility, cylindrical symmetry, and long waveguide lengths. Furthermore, owing to the large Kerr nonlinearity of the materials, fibers with semiconductors embedded in the core are also ideal for the development of integrated nonlinear optical devices. In this paper we review our progress in characterizing the nonlinear transmission properties of the semiconductor optical fibers. Results will be presented for a number of fibers with different core materials, of both crystalline and amorphous forms, which are capable of operating across a broad wavelength range from the visible region up into the mid-infrared. Preliminary demonstrations of nonlinear device functionality will be used to highlight the potential for these fibers to find use in wide ranging applications from signal processing to bio-sensing.

2. FABRICATION

There are two main approaches to fabricating the semiconductor core fibers. The first makes use of a high pressure chemical vapor deposition (HPCVD) method to deposit the materials inside the pores of silica capillaries or microstructured optical fibers (MOFs).[3] This technique is highly flexible in terms of the different materials that can be incorporated into the fiber templates, including both amorphous or crystalline materials from either the unary group IV (silicon and germanium) or compound semiconductor families.[4–6] Furthermore, it can also be adapted to fill capillaries with a range of inner diameters D, as well as microstructured or tapered templates, so that the waveguiding properties can be optimized for specific applications.[7,8] The second approach is based on a more conventional fiber drawing method, called "molten core drawing (MCD)", in which a semiconductor core (particulate or bulk) is sleeved inside a glass cladding tube to form a preform, before being drawn down into a fiber using a tower.[9,10] This technique is more practical in that it is capable of producing much longer lengths of fiber in a single fabrication step, and thus has been more widely adopted by the community.[11–14] The only significant drawback of this method is that the high temperatures used to heat and draw the fiber place some restrictions on the choice of core/cladding material combinations and can also limit the core sizes to be hundreds of microns in diameter due to oxygen contamination. Though this latter issue has been somewhat mitigated recently via the introduction of interfacial modifiers at the core/cladding boundary.[12]

Further author information: (Send correspondence to A.C.P.)
A.C.P.: E-mail: acp@orc.soton.ac.uk

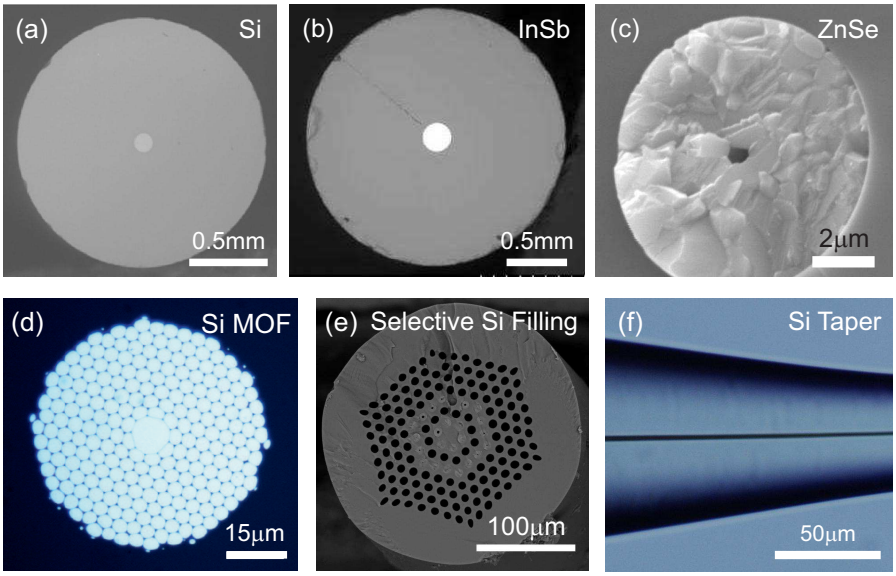

Figure 1. Semiconductor optical fibers. (a) Step-index MCD silicon core fiber, (b) MCD compound (III-V) semiconductor core fiber, (c) HPCVD (II-VI) semiconductor core fiber, (d) HPCVD silicon MOF, (e) HPCVD selectively filled silicon MOF, and (c) tapered silicon core fiber.

Fig. 1 displays an assortment of semiconductor fibers that have been fabricated via the various techniques (MCD and HPCVD). Here Figs. 1(a)-(c) show examples of step-index fibers with (a) silicon (group IV), (b) indium antimonide (III-V), and (c) zinc selenide (II-VI) core materials. Figs. 1(d)-(e) show two different silicon microstructured fibers fabricated by either complete or selective filling of pure silica MOF templates, while Fig. 1(f) is a silicon fiber that has been tapered post-fabrication to vary the core size. Importantly, the fibers displayed on the bottom row demonstrate the capability to tailor the waveguide design far beyond what is achievable on-chip, of particular use for nonlinear applications.[15] As of to date, the lowest optical losses that have been measured for the various core materials are: 0.8 dB/cm for HPCVD hydrogenated amorphous silicon (a-Si:H)[2] and 2 dB/cm for MCD polycrystalline silicon (p-Si) at 1.55 μm,[12] 0.7 dB/cm for MCD Ge at 3.4 μm,[10] and 0.5 dB/cm for HPCVD ZnSe at 2 μm.[6] In terms of their use for nonlinear applications, the greatest progress has been made with silicon core fibers, which will form the focus of this review.

3. NONLINEAR PROPAGATION IN SILICON CORE FIBERS

Nonlinear pulse propagation in the silicon core fibers can be described by a modified form of the nonlinear Schrödinger equation (NLSE), together with a coupled equation for the free carrier density N_c:[16]

$$\frac{\partial A}{\partial z} = -\frac{i\beta_2}{2}\frac{\partial^2 A}{\partial t^2} + i\gamma |A|^2 A - \frac{1}{2}(\sigma_f + \alpha_l) A, \quad (1)$$

$$\frac{\partial N_c}{\partial t} = \frac{\beta_{\mathrm{TPA}}}{2h\nu_0}\frac{|A|^4}{A_{\mathrm{eff}}^2} - \frac{N_c}{\tau_c}. \quad (2)$$

Here A is the pulse envelope, α_l is the linear loss, β_2 is the group velocity dispersion (GVD), and the complex nonlinearity parameter is defined as: $\gamma = k_0 n_2/A_{\mathrm{eff}} + i\beta_{\mathrm{TPA}}/2A_{\mathrm{eff}}$ in terms of the Kerr index (n_2) and two-photon absorption (TPA) coefficient (β_{TPA}), as well as the effective area (A_{eff}). The free carrier (FC) contribution is described by: $\sigma_f = \sigma(1 + i\mu) N_c$ (absorption σ and dispersion μ) and τ_c is the carrier lifetime. To model these equations, the GVD and mode area are estimated via finite element method (FEM) modeling, whilst the loss, nonlinearity and free carrier parameters are determined via transition measurements. It is worth noting that owing to the dB/cm losses of the current generation of fibers, in order to observe nonlinear processes they must be fabricated to have small, few micrometer diameter, core sizes. Thus all of the preliminary measurements of

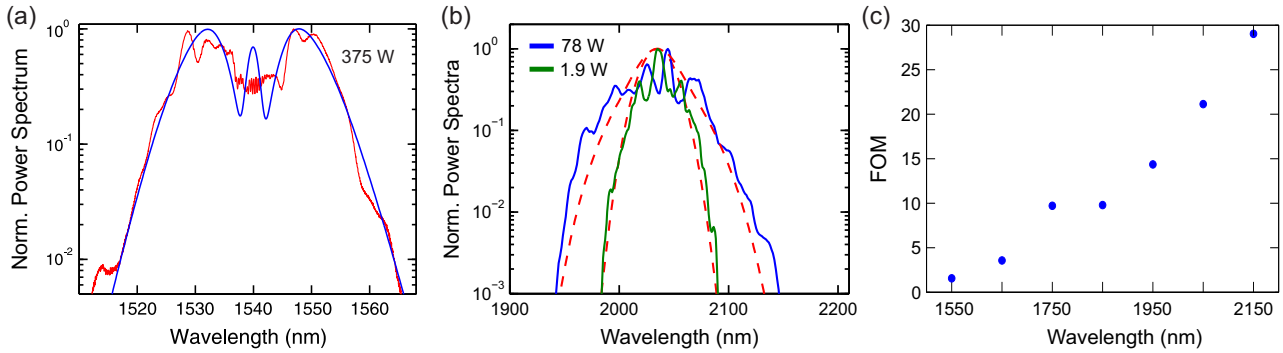

Figure 2. (a) Output spectrum for nonlinear pulse propagation at 1.54 μm together with NLSE fit (coupled power in legend). (b) Output spectra for nonlinear pulse propagation at 2.05 μm together with NLSE fits (coupled powers in legend). (c) Nonlinear FOM as a function of wavelength across the telecom band and up to the edge of the mid-infrared.

the nonlinear propagation in the silicon fibers have been performed with the smaller core HPCVD fabricated fibers and, in particular, those with a-Si:H core materials.

a-Si:H is emerging as an important material for nonlinear photonics as it exhibits low linear losses and a high nonlinearity (up to $\times 5$ larger than crystalline silicon).[17] Furthermore, it also has a comparatively low nonlinear loss parameter which results in a high nonlinear figure of merit, defined as FOM$= n_2/\beta_{\rm TPA}\lambda$. By comparing our measurements of high power pulse propagation with simulations of the NLSE of Eqs. (1) and (2), we have determined the nonlinear parameters for the a-Si:H core fibers. Fig. 2(a) shows the output spectrum for a pulse centered at $\sim 1.55\,\mu$m that has propagated through a $D = 6\,\mu$m core fiber, from which we find the nonlinear parameters to be in the range: $n_2 = 1.5 - 1.8 \times 10^{-13}\,{\rm cm}^2/{\rm W}$ and $\beta_{\rm TPA} = 0.5 - 0.8\,{\rm cm/GW}$, yielding a FOM$\sim 1.5 - 2.4$.[16] More recently, we have extended our characterization beyond the telecoms window and into the short-wave infrared regime, as shown in Fig. 2(b), where we find $n_2 = 1.3 \times 10^{-13}\,{\rm cm}^2/{\rm W}$ and $\beta_{\rm TPA} = 0.03\,{\rm cm/GW}$ at $\lambda = 2.05\,\mu$m. Fig. 2(c) plots the FOM across this region, where we can see that this is even higher (> 20) beyond 2 μm as the n_2 remains large while $\beta_{\rm TPA}$ reduces substantially as the pump wavelength moves across the TPA edge.[18]

4. NONLINEAR PROCESSES IN a-Si:H CORE FIBERS

As a means to benchmark the performance of the fibers in the telecom band, we have conducted a series of simple pump-probe experiments of use for all-optical modulation and switching. Fig. 3(a) shows a spectrogram of a probe pulse centered at 1.59 μm ($T_{\rm fwhm} \sim 800$ fs) under the influence of cross-phase modulation (XPM) induced by a strong pump pulse ($P_p \sim 300$ W) at 1.54 μm ($T_{\rm fwhm} \sim 750$ fs) for different delays.[19] From this it is clear that when the probe propagates alone (large delays) the spectral components are unaltered, whilst in the presence of the pump the peak spectral wavelength, shown by the white dashed line, is red (blue) shifted for positive (negative) delays. It is clear from this image that the switching occurs on a femtosecond timescale, and we note that the asymmetry in the wavelength conversion is simply due to TPA (from the telecom pump) and thus could be reduced by moving either to longer wavelengths or shorter pulse durations. Nevertheless, the large 10 nm red shift is sufficient to yield an extinction ratio of 12 dB, suitable for use in an array of ultrafast modulation and switching applications.

To illustrate the benefits of the large FOM of a-Si:H around the 2 μm region, Fig. 3(b) shows the first observation of supercontinuum generation in a semiconductor core fiber.[20] These results were obtained by using a smaller core fiber ($D \sim 2\,\mu$m) and moving the pump source to longer wavelengths (beyond the TPA edge) to access a region of lower nonlinear loss. More significantly, for this fiber the zero dispersion wavelength was $\lambda_z \sim 2.1\,\mu$m so that it was possible to access the anomalous dispersion regime, where the spectral broadening can be enhanced through phase-matched four-wave mixing and soliton fission.[21] The largest continuum spanning more than an octave ($1.64 - 3.37\,\mu$m) was recorded for the longer pump wavelength, which we attribute in part to the lower linear losses that were measured at 2.5 μm ($\sim 0.4\,{\rm dB/cm}$). It is worth noting that when pumping

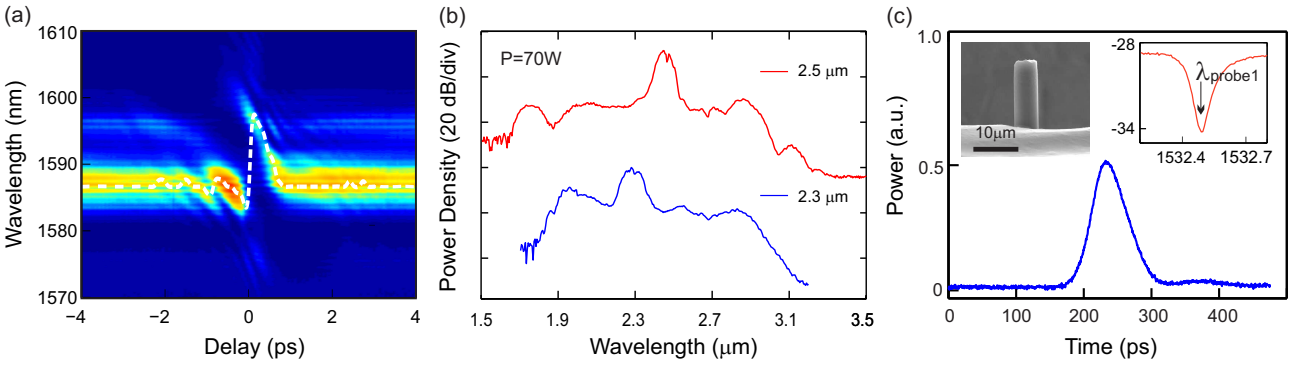

Figure 3. a-Si:H core fibers for optical processing. (a) Spectrogram of cross-phase modulation; dashed white line indicates the peak wavelength shifting. (b) Supercontinuum spectra generated in a small core silicon fiber when pumped in the anomalous dispersion regime; central pump wavelengths as labeled. (c) All-optical on/off switching of a CW probe circulating in a silicon fiber-based resonator (see left hand inset), induced by a picosecond pulsed pump. The right hand inset shows the CW probe position with respect to cold cavity resonance dip.

in the normal dispersion regime with $\lambda = 1.85\,\mu$m, the largest measured broadening was only 700 nm (< 0.7 of an octave). Thus these results motivate a shift to investigate the use of these a-Si:H core fibers further into the mid-infrared region.

Although the results of Fig. 3(a)-(b) were obtained with pump power levels that are much lower than those required for nonlinear pulse propagation in silica fibers, it is possible to reduce the power thresholds even further by using the fibers in a resonator geometry. Whispering gallery mode (WGM) resonators with high quality factors (Q) and small mode volumes are becoming increasingly popular for nonlinear applications, and the large n_2 and tight mode confinement in the silicon structures greatly enhances the nonlinear effects compared to their silica fiber counterparts.[22] The left hand inset of Fig. 3(c) shows an a-Si:H fiber resonator fabricated by etching away the silica cladding. For a material loss of 1.5 dB/cm at 1.54 μm the loaded Q factors are of the order $Q_l \sim 2 \times 10^4$. By characterizing the nonlinear effects in a resonator with a 6 μm diameter, we have measured large Kerr resonance wavelength shifts of ~ 3 nm when pumping with short pump pulses of only $P_{ave} \sim 20\,\mu$W ($P_p \sim 20$ mW).[23] These large Kerr shifts occur on an ultrafast time scale so that they can be readily exploited for all-optical processing using a pump-probe configuration. Fig. 3(c) shows the on/off switching of a CW signal when pulsed pump light is coupled into the resonance, as shown in the right hand inset. Significantly, the optical modulation was realized at switching thresholds as low as $\sim 5\,\mu$W ($P_p \sim 5$ mW), up to four orders of magnitude lower than previous transmission-based experiments in Fig. 3(a).

5. NONLINEAR PROCESSES IN ZINC SELENIDE CORE FIBERS

One of the drawbacks of silicon for nonlinear optics is that the processes are limited to those based on the third order $\chi^{(3)}$ susceptibility. Thus the possibility to access the larger $\chi^{(2)}$ susceptibility in crystalline compound semiconductor core fibers is highly advantageous, not only for the potential to reduce the power thresholds, but also as it allows for the observation of processes such as second harmonic generation (SHG). In Fig. 4(a), we present the first observation of a visible (red) second harmonic signal generated in a ZnSe core fiber when it is pumped with a telecoms source.[24] In order to satisfy phase matching, the fiber was pumped in a WGM geometry, similar to that shown in the inset of Fig. 3(c). The corresponding transmission spectrum for the resonator in the vicinity of the pump wavelength is shown in the inset of Fig. 4(a), with the resonance into which the pump was coupled highlighted in red. We note that this resonance has a load Q factor of $\sim 10^3$, which corresponds to a linewidth of ~ 0.2 nm. Taking this into consideration, the position of the generated second harmonic light is in excellent agreement with the pump resonance at 1548 nm, i.e., $\lambda_s = 1548/2 \sim 773.9$ nm. Furthermore, no other emission lines were observed within the range of the spectrometer ($350 - 1700$ nm), indicating that SHG was the dominant nonlinear process.

To confirm the second harmonic nature of the process, Fig. 4(b) shows a logarithmic plot of the collected second harmonic power (P_s^{out}) as a function of the power dropped into the resonator (P_p^{in}), where it can be

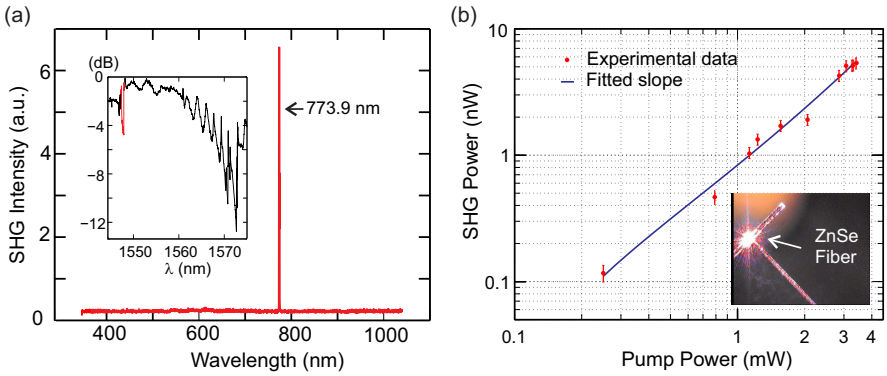

Figure 4. (a) Measured emission second harmonic spectrum; inset displays the corresponding transmission spectrum showing the pump resonance at $\lambda \sim 1548\,\text{nm}$ red fit). (b) Log-log plot of measured second harmonic power as a function of the fundamental power dropped into the resonator; solid line is a linear fit with an expected slope of ~ 2. Inset shows a photograph of the generated visible second harmonic light.

seen that the minimum coupled power at which we recorded a measurable harmonic signal was $250\,\mu\text{W}$. Fitting the data with a linear curve we obtain a slope of 1.95 ± 0.10, which is in good agreement with the expected quadratic dependence. Using this value we can then extract the external efficiency as $\eta_{\text{ext}} = P_s^{\text{out}}/(P_p^{\text{in}})^2 = (8.8 \pm 0.4) \times 10^{-4}\,\text{W}^{-1}$, which is comparable to what has been obtained in GaAs-based micro-disks fabricated on-chip.[25] It is also worth noting that in contrast to previous reports, our measurements do not show any evidence of a roll-off in second harmonic power associated with thermal shifting of the pump resonance. We attribute this behaviour to the order of magnitude lower thermo-optic coefficient of the ZnSe material compared to GaAs, which makes it more suitable for high power pumping.

6. CONCLUSION

Semiconductor fibers with various core materials and waveguide designs have been fabricated via chemical deposition and fiber drawing methods. Both these methods are now sufficiently advanced that the semiconductor fibers are regularly produced with optical transmission losses as low as a few dB/cm, which is enabling the first nonlinear characterizations and device demonstrators. The results presented in this paper show that these fibers are a suitable platform for the development of nonlinear optical devices covering a broad wavelength range from the visible region up in to the mid-infrared.

6.1 Acknowledgments

The authors acknowledge their colleagues that have contributed to this work, including Dr P. Mehta, Dr T. Day, Dr J. Sparks, Dr P. Horak, and Prof. J. Badding. Financial support has been provided by EPSRC (EP/G051755/1, EP/I035307/1, EP/J004863/1).

REFERENCES

[1] Ballato, J., Hawkins, T., Foy, P., Yazgan-Kokuoz, B., McMillen, C., Burka, L., Morris, S., Stolen, R., and Rice, R., "Advancements in semiconductor core optical fiber," *Opt. Fiber Technol.* **16**, 399 (2010).

[2] Peacock, A. C., Sparks, J. R., and Healy, N., "Semiconductor optical fibres: progress and opportunities," *Laser Photon. Rev.* **8**, 53 (2014).

[3] Sazio, P. J. A., Amezcua-Correa, A., Finlayson, C. E., Hayes, J. R., Scheidemantel, T. J., Baril, N. F., Jackson, B. R., Won, D.-J., Zhang, F., Margine, E. R., Gopalan, V., Crespi, V. H., and Badding, J. V., "Microstructured optical fibers as high-pressure microfluidic reactors," *Science* **311**, 1583 (2006).

[4] Lagonigro, L., Healy, N., Sparks, J. R., Baril, N. F., Sazio, P. J. A., Badding, J. V., and Peacock, A. C., "Low loss silicon fibers for photonic applications," *Appl. Phys. Lett.* **96**, 041105 (2010).

[5] Mehta, P., Krishnamurthi, M., Healy, N., Baril, N. F., Sparks, J. R., Sazio, P. J. A., Gopalan, V., Badding, J. V., and Peacock, A. C., "Mid-infrared transmission properties of amorphous germanium optical fibers," *Appl. Phys. Lett.* **97**, 071117 (2010).

[6] Sparks, J., He, R., Healy, N., Krishnamurthi, M., Peacock, A. C., Sazio, P. J. A., Gopalan, V., and Badding, J. V., "Zinc selenide optical fibers," *Adv. Mater.* **23**, 1647 (2011).

[7] Healy, N., Sparks, J. R., Petrovich, M. N., Sazio, P. J. A., Badding, J. V., and Peacock, A. C., "Large mode area silicon microstructured fiber with robust dual mode guidance," *Opt. Express* **17**, 18076 (2009).

[8] Healy, N., Sparks, J. R., Sazio, P. J. A., Badding, J. V., and Peacock, A. C., "Tapered silicon optical fibers," *Opt. Express* **18**, 7596 (2010).

[9] Ballato, J., Hawkins, T., Foy, P., Stolen, R., Kokuoz, B., Ellison, M., McMillen, C., Reppert, J., Rao, A. M., Daw, M., Sharma, S., Shori, R., Stafsudd, O., Rice, R. R., and Powers, D. R., "Silicon optical fiber," *Opt. Express* **16**, 18675 (2008).

[10] Ballato, J., Hawkins, T., Foy, P., Morris, S., Hon, N. K., Jalali, B., and Rice, R., "Silica-clad crystalline germanium core optical fibers," *Opt. Lett.* **36**, 687 (2011).

[11] Scott, B., Ke, W., and Pickrell, G., "Fabrication of n-type silicon optical fibers," *Photon. Technol. Lett.* **21**, 1798 (2009).

[12] Nordstrand, E., Dibbs, A., Eraker, A., and Gibson, U. J., "Alkaline oxide interface modifiers for silicon fiber production," *Opt. Mater. Express* **3**, 651 (2013).

[13] Hou, C., Jia, X., Wei, L., Tan, S.-C., Zhao, X., Joannopoulos, J., and Fink, Y., "Crystalline silicon core fibres from aluminium core preforms," *Nat. Comm.* **6**, 6248 (2015).

[14] Zhang, S., Zhao, Z., Chen, N., Pang, F., Chen, Z., Liu, Y., and Wang, T., "Temperature characteristics of silicon core optical fiber Fabry-Perot interferometer," *Opt. Lett.* **40**, 1362 (2015).

[15] Peacock, A. C., "Soliton propagation in tapered silicon core fibers," *Opt. Lett.* **35**, 3697 (2010).

[16] Mehta, P., Healy, N., Baril, N. F., Sazio, P. J. A., Badding, J. V., and Peacock, A. C., "Nonlinear transmission properties of hydrogenated amorphous silicon core optical fibers," *Opt. Express* **18**, 16826 (2010).

[17] Grillet, C., Carletti, L., Monat, C., Grosse, P., Bakir, B. B., Menezo, S., Fedeli, J. M., and Moss, D. J., "Amorphous silicon nanowires combining high nonlinearity, FOM and optical stability," *Opt. Express* **20**, 22609 (2012).

[18] Shen, L., Healy, N., Mehta, P., Day, T. D., Sparks, J. R., Badding, J. V., and Peacock, A. C., "Nonlinear transmission properties of hydrogenated amorphous silicon core fibers towards the mid-infrared regime," *Opt. Express* **21**, 13075 (2013).

[19] Mehta, P., Healy, N., Day, T. D., Badding, J. V., and Peacock, A. C., "Ultrafast wavelength conversion via cross-phase modulation in hydrogenated amorphous silicon optical fibers," *Opt. Express* **20**, 26110 (2012).

[20] Shen, L., Healy, N., Xu, L., Cheng, H. Y., Day, T. D., Price, J. H. V., Badding, J. V., and Peacock, A. C., "Four-wave mixing and octave-spanning supercontinuum generation in a small core hydrogenated amorphous silicon fiber pumped in the mid-infrared," *Opt. Lett.* **39**, 5721 (2014).

[21] Genty, G., Coen, S., and Dudley, J. M., "Fiber supercontinuum sources," *J. Opt. Soc. Am. B* **24**, 1771 (2007).

[22] Pöllinger, M. and Rauschenbeutel, A., "All-optical signal processing at ultra-low powers in bottle microresonators using the Kerr effect," *Opt. Express* **18**, 17764 (2010).

[23] Vukovic, N., Healy, N., Suhailin, F. H., Mehta, P., Day, T. D., Badding, J. V., and Peacock, A. C., "Ultrafast optical control using the Kerr nonlinearity in hydrogenated amorphous silicon microcylindrical resonators," *Sci. Rep.* **3**, 2885 (2013).

[24] Vukovic, N., Healy, N., Sparks, J. R., Badding, J. V., Horak, P., and Peacock, A. C., "Tunable continuous wave emission via phase-matched second harmonic generation in a ZnSe microcylindrical resonator," *Sci. Rep.* **5**, 11798 (2015).

[25] Mariani, S., Andronico, A., Lemaître, A., Favero, I., Ducci, S., and Leo, G., "Second-harmonic generation in AlGaAs microdisks in the telecom range," *Opt. Lett.* **39**, 3062 (2014).